Iterative Redeployment of Illumination and Sensing (IRIS): Application to STW-SAR Imaging

Jay Marble[†,*], Raviv Raich[*], Alfred O. Hero[*]
[†]Night Vision Laboratory, Fort Belvoir, VA 22060
[*]University of Michigan, Ann Arbor, MI 48109-2122

***Abstract*— A new technique which we call Iterative Redeployment of Illumination and Sensing (IRIS) is introduced and applied to See-Through-the-Wall radar imaging. IRIS is applicable to adaptive sensing scenarios where the medium is illuminated and measured multiple times using different illiminator/sensor configurations, e.g., position, bandwidth, or polarization. These configurations are adaptively selected to minimize uncertainty in the image reconstruction. The IRIS algorithm has the following features: (1) use of a sparse Bayesian image model that captures the free-space dominated propagation characteristics of interiors of man-made structures such as caves and residences; (2) iterative reconstruction of both an image and an image confidence map from the posterior likelihood in the form of a thresholded Landweber recursion, (3) use of the Bayesian model to predict the best redeployment configuration of the illuminator platform given the current image and confidence map. For the STW application we approximate the forward operator by a matrix formulation of wavenumber migration. A simulated STW application is provided that illustrates the IRIS algorithm.**

I. Introduction

Imaging with See-Through-the-Wall (STW) radar is of high interest to military, homeland security, and search-and-rescue operations due to its ability to provide information on activities and conditions behind walls. Tracking suspicious individuals, detection of weapons caches, layout mapping, and fire rescue are examples of STW applications. For such applications STW radar must have the following properties: rapid deployment, small (even portable) size, and the ability to perform fast image reconstruction from limited angle views. In general, to maximize resolution and signal-to-noise performance one should deploy as powerful a radar as possible, i.e., high transmit energy and long baseline. However, in military, homeland security, or firefighting applications, the deployment of bulky or long-baseline STW radar platforms might entail risks that could compromise mission objectives or endanger those who are deploying the radar. In these situations, it is essential that the size of the illumination and sensing platforms be small and that the radar deployment time, e.g., the baseline of a SAR system, be short. To gain back some of the performance lost by downsizing the radar we propose an adaptive deployment strategy that we call iterative redeployment of illumination and sensing (IRIS). IRIS allows one to rapidly learn the propagation environment, adapt the configuration of the radar, e.g., its placement at the exterior of a building, and continuously improve the image during the deployment process.

One unique characteristic of STW that the IRIS approach exploits is that in man-made structures most of the image volume is empty space, i.e., interiors are only sparsely populated with scatter centers. This allows us to implement fast image reconstruction and derive an image confidence map that measures the degree of uncertainty that a scatterer exists at any specified location in the image. Regions of the image with high uncertainty may need to be reimaged with a different illumination/sensor configuration. The optimal redeployment configuration, e.g., sensor position, can be determined on the fly by choosing the one that would maximize information gain in interesting regions of the image where scatterer confidence, as predicted by the confidence map, is low. Information gain is computed by placing a virtual emitter in the low confidence region and applying the reciprocity principle. This forms the basis for the IRIS approach.

The elements of the IRIS approach are illustrated in Fig. 1 and 2. The former figure illustrates the iterations over the block operation in 2. The algorithm starts with an initial position of the sensor/illuminator and an initial estimate of the image, which could be very crude, e.g., an all blank image, or could use prior information, e.g.,

This research was partially supported by the Army Research Office, grant number DAAD19-02-1-0262. Authors can be contacted at {jamarble,ravivr,hero} at umich.edu

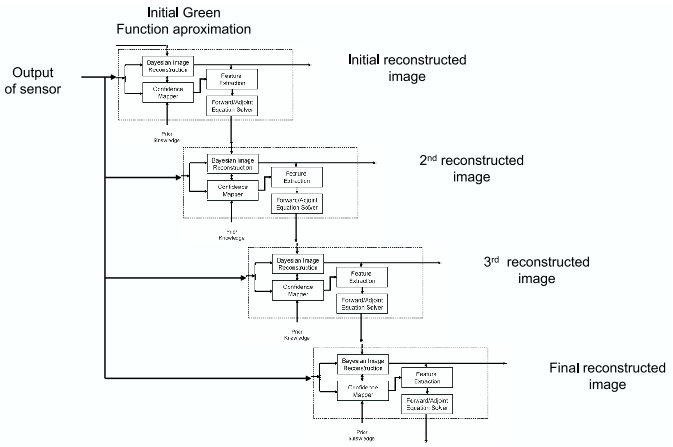

Fig. 1. Block diagram of IRIS algorithm iterated over the core operation illustrated in Fig. 2.

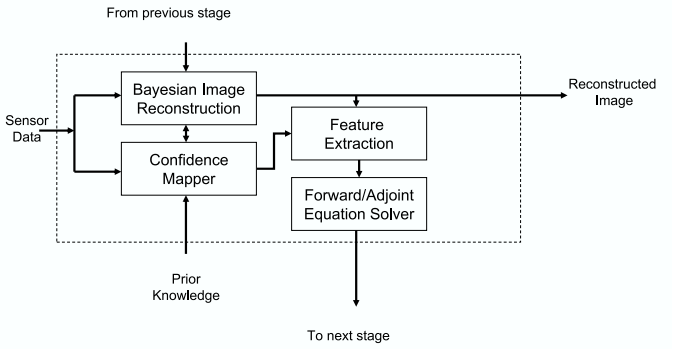

Fig. 2. Block diagram of the core operation in the IRIS algorithm.

building interior wall layout. using an iterative Bayesian MAP estimation strategy, the initial image is combined with the SAR measurements data in a "backprojection step" (involving the adjoint of the Greens function and computed via EM iterations in (1)) that produces an updated image and an approximate image confidence map (expression (3)). The confidence map is used to select regions of the image that could not be reconstructed with high confidence from the SAR measurements. Features extracted from the confidence image are used to estimate likely positions of scatterers and approximate the "forward projection" (Greens function) characterizing wave propagation inside the building. The induced information gain field over possible sensor/illuminator redeployment configurations (expression (4) is simulated using this Greens function when a virtual transmitter is placed in a region of the image having low confidence). This information gain field is used to select among candidate positions for redeployment and the same operation is applied to the new image, confidence map, and redeployed sensor/illuminator data.

The outline of the paper is as follows. In Sec. II we describe the Bayesian iterative image reconstruction algorithm using a linear model. Each iteration involves application of a forward channel matrix and an adjoint channel matrix to the most recent reconstructed image and predicted measurement residual, respectively. In this section we introduce induce sparseness inducing priors for reconstruction of the image and confidence map on scatterer locations in the image. In Sec III we introduce a fast "reverse wavenumber migration" approximation to the forward and adjoint operators that uses 2D FFTs, phase correction, and interpolation. In Sec. IV we describe the information gain metric that IRIS uses to adapt the illumination to mitigate regions of poor confidence. Finally, in Sec. V we show simulation results for a STW SAR application and conclude in Sec VI.

II. Image Reconstruction and Scatterer Probability Mapping

Most image reconstruction approaches can be interpreted as solutions to a cost function minimization problem, e.g., minimization of the sum of squared residual errors between the observed measurements and measurements synthesized with a candidate reconstructed image. The starting point is the linear vector measurement model $Y = HX+N$, where Y is a vector of radar return amplitudes measured over time and/or space, H is the transfer function, or forward operator matrix, associated with the medium, X is the vectorized image or scene, and N is a vector of residual errors associated with assuming the linear model.

For a candidate image X the sum of squared residuals cost function is $L(X) = \|Y - HX\|^2$ where "$\|\cdot\|$" denotes the Euclidean norm. The least squares image reconstruction algorithm minimizes $L(X)$ and is given by the closed form expression (assuming that matrix H is full column rank)

$$\hat{X} = [H^T H]^\dagger H^T Y,$$

where H^T is the hermitian transpose, also called the adjoint matrix, of H and $[H^T H]^\dagger$ is the pseudoinverse of the matrix $H^T H$. The forward operator H and its hermitian transpose are fundamental to this imaging approach and Sec. 3 describes an approximation to these matrices for radar imaging applications.

When prior information, e.g., smoothness or sparsity, on properties of the image is available a Bayesian image reconstruction approach is justified. Let $f(X)$ be a density function that captures this prior information and assume that the model error residual N is a vector of independent identically distributed (i.i.d.) Gaussian random variables with zero mean and variance σ^2, The

maximum a posteriori (MAP) reconstruction maximizes the posterior density $f(X|Y) = f(Y|X)f(X)/f(Y)$ or equivalently minimizes the objective function

$$L(X) = \|Y - HX\|^2/(2\sigma^2) + \log f(X)$$

Only in rare cases, e.g., Gaussian $f(X)$, is the minimizer of $L(X)$ available in closed form. However, this MAP reconstruction can always be implemented iteratively using the Expectation-Maximization (EM) algorithm [1]. As shown in [2] the EM algorithm performs image reconstruction by iterating two nested operations the "E" (deconvolution) step and the "M" (denoising) step:

$$\begin{aligned} (E)\ \ \hat{Z}^{(n)} &= \hat{X}^{(n)} + \alpha H^T(Y - H\hat{X}^{(n)}) \\ (M)\ \ \hat{X}^{(n+1)} &= \arg\min_X \Big(\frac{\|\hat{Z}^{(n)} - X\|^2}{2\sigma^2} + \log f(X) \Big). \end{aligned} \tag{1}$$

A. Sparse Bayesian image model

We adopt a model for the joint image density $f(X)$ that reflects inherent sparseness (many zero entries in the vector X) introduced in [3] for molecular imaging applications. As we will see this model also yields a confidence map estimate. Adopting the notation $X = [x_1, \ldots, x_P]^T$ the model is $f(X) = \prod_{i=1}^P g(x_i)$ where g is the marginal density

$$g(x) = (1-w)\delta(x) + \frac{wa}{2} e^{-a|x|} \tag{2}$$

$\delta(x)$ is a dirac delta function (point mass at zero), $w \in [0,1]$, $a > 0$ are parameters, which are generally unknown and must be estimated. With this model the EM algorithm (1) gives an M step, which is closed form and is equivalent to applying a soft thresholding function to each of the variables $\hat{Z}^{(n)}$ [3]. Furthermore, this model gives an iterative approximation to the posterior probability $P(x_i = 0|Y)$ that the i-th pixel is zero [4]:

$$\begin{aligned} P(x_i = 0|Y) &\approx \frac{\frac{1-w}{\sqrt{2\pi\sigma^2}} e^{-\frac{z^2}{2\sigma^2}}}{f_z(z)} \\ f_z(z) &= \frac{1-w}{\sqrt{2\pi\sigma^2}} e^{-\frac{z^2}{2\sigma^2}} + A(w,a,\sigma,z) + B(w,a,\sigma,z), \end{aligned} \tag{3}$$

where

$$\begin{aligned} A(w,a,\sigma,z) &= \frac{aw}{4}\big(1 - \mathrm{erf}\big(\frac{a\sigma + \frac{z}{\sigma}}{\sqrt{2}}\big)\big) e^{\frac{a^2\sigma^2 + 2az}{2}}, \\ B(w,a,\sigma,z) &= \frac{aw}{4}\big(1 + \mathrm{erf}\big(\frac{\frac{z}{\sigma} - a\sigma}{\sqrt{2}}\big)\big) e^{\frac{a^2\sigma^2 - 2az}{2}}. \end{aligned}$$

An image of the values of $P(x_i = 0|Y)$ over all pixel indices i will be called the "probability map" of scatterers in the reconstructed image.

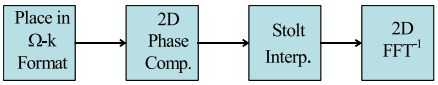

Fig. 3. Block diagram of wavenumber migration. The SAR measurements Y are input to the block at the left of diagram and the reconstructed image X is output at the block on the right.

III. Reverse migration approximation

The form of the matrices H and H^T in the EM iteration (1) will depend on the specific application and modality used to illuminate and sense the environment. For SAR imaging we develop an approximation to these matrices that is based on a matrix formulation of wavenumber migration. Wavenumber migration was first developed as a way of imaging seismic data for oil exploration. It was applied to synthetic aperture radar imaging in the early 90s. [5]. Wavenumber migration is implemented by rebinning the frequency-wavenumber spectrum ($\Omega - k$ domain) into a 2D Fourier spectrum plus a correction factor determined by a Stolt interpolation [6].

Wavenumber migration can be interpreted as composition of several operators, which can implemented as a sequence of matrix operations (See block diagram in Fig. 3). This gives a compact mathematical form for the image reconstruction $X = \Psi Y$ where

$$\Psi = Q_2^{-1} \Phi Q_1,$$

and Q_1 is a 1D FFT, placing the observations into the frequency-wavenumber ($\Omega - k$) space. Q_2 is the matrix implementation of a 2D FFT and the phase compensation and Stolt interpolation and are folded into the matrix Φ. The matrix Ψ an be identified as an approximation to the pseudo-inverse $[H^T H]^{-1} H^T$ of the forward operator H.

The Stolt interpolation is a 1D interpolation between sampled frequencies in the wavenumber domain. To implement this operation as a matrix we start with the simple two point (linear) interpolator. If we denote the set of observations by $y[n,m]$ where n corresponds to the n-th spatial location along the synthetic aperture and m corresponds to the m-th transmitted frequency, then the Stolt interpolation can be written as $y[n,m] \rightarrow a_m y[n,m] + b_m y[n[m+1]$ for frequency dependent interpolation coefficients a_m, b_m:

$$a_m = \frac{k'_m - k_m}{k_{m+1} - k_m}, \quad b_m = \frac{k_{m+1} - k'_m}{k_{m+1} - k_m}$$

corresponding to a vector interpolation of the form $Y \rightarrow AY$ where A is a sparse matrix. Here $k_m = 2\pi f_m / c$ is the wavenumber at the m-th frequency and k'_m is the wavenumber at m-th interpolated frequency.

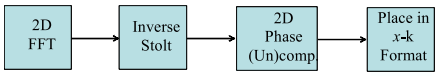

Fig. 4. Block diagram of reverse wavenumber migration approximation to the forward operator H. The image X is input to the block at the left of diagram and the SAR measurements Y are output at the block on the right.

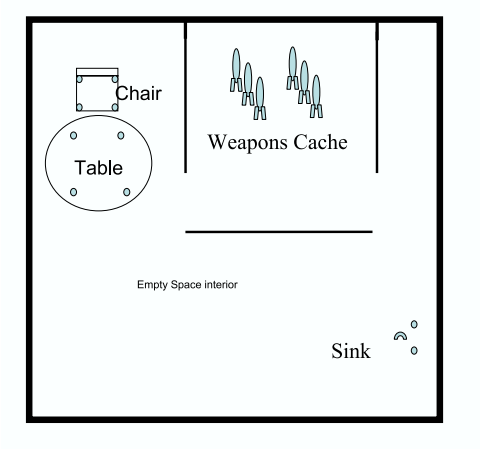

Fig. 5. 2D scenario used to illustrate the IRIS approach. Room is 10×10 meters and a SAR sensor with 1 meter baseline can be placed at any position parallel to top or bottom walls at exterior of building.

The phase correction component of the matrix Φ is accomplished by adjusting the a_m and b_m coefficients according to [7] $a_m \rightarrow a_m e^{-j(k_m - k'_m)R_s}$ and $b_m \rightarrow a_m e^{-j(k_{m+1} - k'_m)R_s}$, where R_s is the slant range from the scene center to the aperture. Thus Φ can be represented as the matrix composition $\Phi_s = BA$ where B is diagonal. Thus wavenumber migration takes the form of a matrix composition $\Psi = Q_2^{-1} B A Q_1$ of circulant, diagonal, and sparse matrices. A reverse wavenumber migration approximation to the forward operator H can be extracted by computing the inverse of Ψ resulting in: $H = Q_1^{-1} A^{-1} B^{-1} Q_2$, which is illustrated in the block diagram of Fig. 4.

Note that the while the Stolt matrix A is sparse the inverse Stolt matrix A^{-1} is not sparse. However, by using linear equation solvers of the form $X = \Psi Y$ instead of matrix inversion the reverse migration operator $HX = \Psi^{-1} X$ can still be implemented in (1) using sparse computations.

IV. IRIS Adaptation via information gain

Assume an initial sensor/illuminator configuration has been deployed and that an image has been reconstructed along with its confidence map using the iterative Bayesian algorithm described in Sec. II. The objective of IRIS is to find a new sensor configuration that will allow us to improve upon the initial reconstructed image. For concreteness, we focus on imaging the interior of a building and assume that the space of possible configurations are locations where the baseline of a small SAR sensor could be placed at the building exterior (see Fig. 5). The proposed IRIS approach uses the confidence map to identify regions of the image that were poorly resolved, i.e., pixels that have poor confidence values ($P(x_i = 0|Y)$ near 0.5). It then simulates the RF field at the building exterior that would be created by placing a (virtual) transmitter in one of the poor confidence regions of interest. From this simulated field we can extract information about the best location to redeploy the illumination/sensing platform.

For this purpose we define the predicted information gain as a measure of how much a given sensor position might enhance the ability to detect the presence or absence of a scatterer in the vicinity of the virtual transmitter. The value of redeploying the sensor at a particular location can be measured by the variation of the RF field at that location produced by perturbing the location of the virtual transmitter. Define the energy frequency spectrum $E_{x,y}(\omega)$ of the RF field measured at location y due to an omnidirectional transmitter placed at location x, and for a location x_k define $E_k = E_{x_k,y}$. The spectral variation produced by perturbing the location x from a reference location x_1 to a new location x_2 can be measured by the Kullback-Liebler (KL) divergence

$$D(E_1 \| E_2) = \int E_1(\omega) \log \left(\frac{E_1(\omega)}{E_2(\omega)} \right) d\omega.$$

The KL divergence and its generalizations have been used by many authors in sensor management problems and are often referred to as the information gain [8]–[10]. We define the information gain at sensor position y as the sum of the KL divergences of the RF fields produced by cross-range perturbation $x_1 \rightarrow x_2$ and range perturbation $x_1 \rightarrow x_3$ of the virtual transmitter location:

$$\overline{\mathrm{IG}}(x, y) = D(E_1 \| E_2) + D(E_1 \| E_3). \quad (4)$$

When viewed as a function of y this quantity sweeps out the information gain field.

V. Numerical Simulation

We consider a scenario illustrated in Fig. 5. A weapons cache is hidden in a room surrounded by four exterior walls and obscured by other interior walls and objects in the room. A mono-static radar can be placed anywhere above the top wall or below the bottom wall. The room is enclosed by a 10×10 meter wall that is 1/3 meter thick. We evaluate the performance of a short baseline (1 meter) SAR sensor that can be placed at any position along the 10 meters of the top or bottom wall

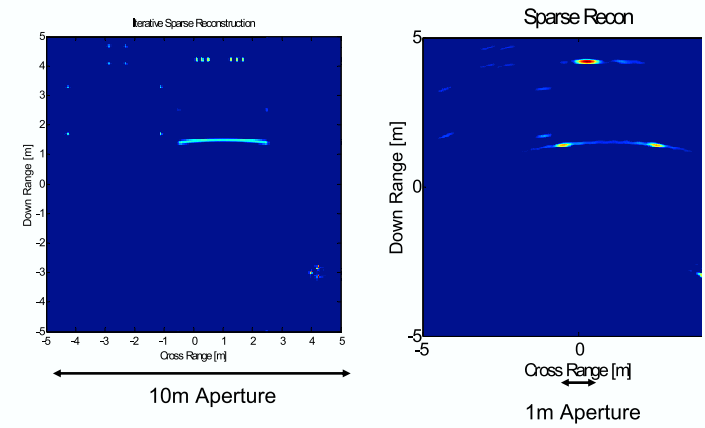

Fig. 6. Iterative reconstruction of building interior illustrated in Fig. 5 after 10 iterations and a full 10 meter baseline (left) and 1 meter baseline (right) monostatic SAR illuminator/sensor.

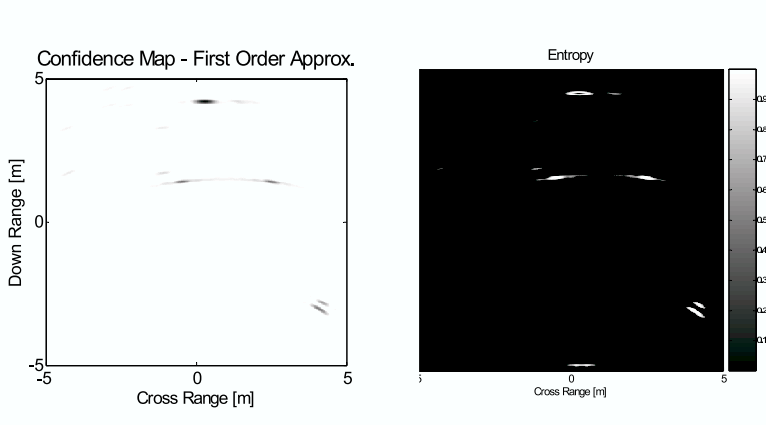

Fig. 7. confidence map (left) and entropy map (right) associated with the 1 meter baseline image reconstruction shown in Fig. 6.

at 1 meter standoff distance. The operating frequency of the simulated radar was 4.0GHz to 5.0GHz and the SAR radar baseline was sampled at 10 points (every 10cm) along its 1 meter extent. The simulator modeled each object on the room with a simple superposition of dyhedral (spell: dihedral???) scatterers using physical optics. We assume that the external wall attenuation and phase parameters are accurately estimated, e.g using the method of [11].

For an initial sensor position centered at the middle of the lower wall the two panels of Fig. 6 show the results of applying ten iterations of the Bayesian iterative reconstruction algorithm (1) with sparseness prior (2). The values of a, w and σ were fixed during the entire experiment. The right panel of the figure is significantly lower resolution than the left panel due to its relatively smaller baseline of 1 meter. The left panel is the reconstruction obtained after the first iteration of the IRIS procedure.

The probability map $P(x_i = 0|Y)$ and the associated entropy map $-\log P(x_i = 0) - \log P(x_i = 1)$ are shown in Fig. 7. The entropy map is maximum for reconstructed pixels whose *a posteriori* probability of being empty space is close to 1/2. The entropy map therefore measures the *a posteriori* (lack of) confidence in the value of that pixel and is called the "confidence map" of the image. From the confidence map a region of low confidence is identified, e.g., the region near the top of the image, and a virtual emitter is simulated in this region to generate an information gain field for determining the best redeployment configuration for the next iteration of IRIS.

The construction of the information gain field is illustrated in Fig. 8 for the scenario illustrated in Fig. 5

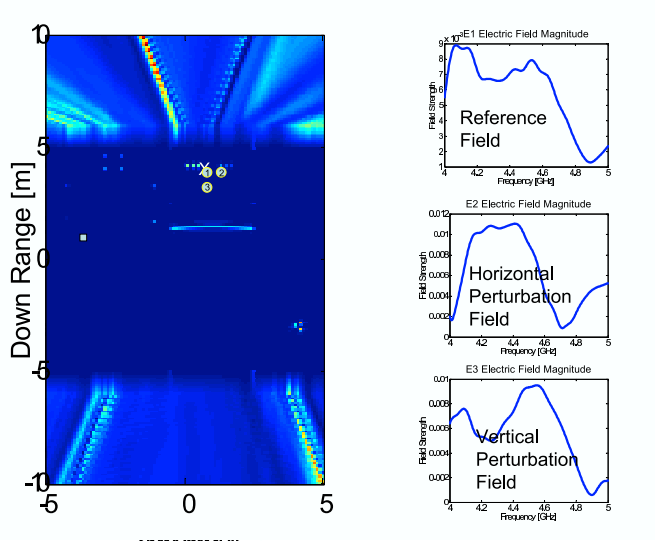

Fig. 8. The information gain field is computed by simulating the variability of the RF spectrum that a virtual transmitter in the vicinity of a pixel of interest (circle 1 in left panel) would generate at different locations at the exterior of the building. At right are the induced RF fields generated by a virtual transmitter at the reference position (circle 1), cross-range (circle 2), and range (circle 3) perturbations.

and a low confidence region region identified from Fig. 7. On the right of the figure is the frequency spectrum of the induced RF field at a candidate redeployment position at the exterior of the building for the three sensor positions illustrated in the left panel of the figure. The difference between the reference spectrum and the horizontally (cross-range) and vertically (range) perturbed spectra is measured via the information gain formula (4). On the left of Fig. 8 at the exterior of the building is the color coded field corresponding to the information gain. The distances of the range and cross-range perturbations of the virtual transmitter have been exaggerated for clarity of presentation; actual perturbations would produce less obvious visual differences in the RF spectra.

In Fig. 9 the virtual transmitter positions and induced

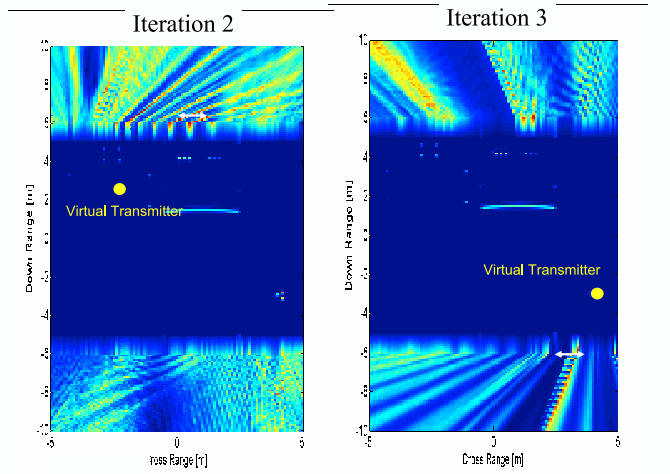

Fig. 9. Virtual transmitter locations and the induced information gain fields for iteration 2 and 3 of IRIS for the scenario illustrated in Fig. 5.

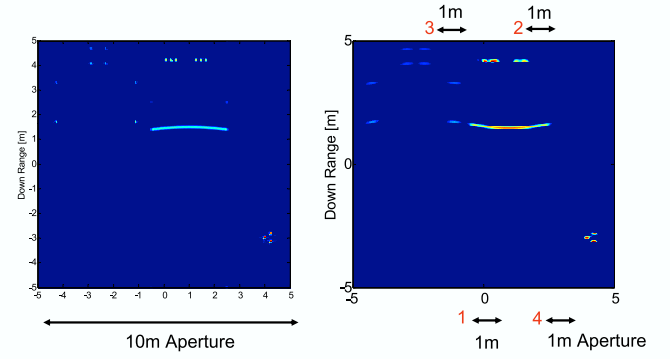

Fig. 10. Comparison between final IRIS reconstruction after 4 iterations with 1 meter baseline SAR deployments (shown by black arrows) versus one shot IRIS reconstruction using 10 meter baseline. In both cases the reverse wavenumber migration model with EM implementation of MAP algorithm has been used.

information gain fields are illustrated for iteration 2 and 3 of the IRIS algorithm. Optimal information gain maximizing SAR positions are indicated by the 1 meter baseline white arrows at exterior of the building. After the third iteration of IRIS 4 different sensor positions will have been deployed (including the initial deployment).

On the right panel of Fig. 10 a composite of the four reconstructed images (including the final image) obtained from the three iterations of the adaptive IRIS algorithm described above. The recovered resolution using IRIS's total baseline of 4 meters is comparable to the resolution of the non-adaptive one-shot 10 meter baseline shown on the left panel of the figure.

VI. Conclusions

We presented a new Bayesian iterative approach called IRIS which allows one to sequentially place sensor and illuminators around a building in a manner that successively maximizes the information gain in poorly resolved regions of the image of the building interior. The algorithm works adaptively in four steps: (i) It observes the scene at an initial location and creates a scattering model of the building (i.e., the environment). (ii) It generates a confidence map of the locations of scatterers to reveal poorly-measured areas of the scene based on the acquired observations. (iii) It places virtual transmitters at locations of uncertainty in the scene and utilizes numerical electromagnetic simulations to compute the electric fields exiting the building. (iv) It uses an information gain criteria to determine the next sensor redeployment configuration. In this way a high quality image is formed adaptively from the observations. The IRIS algorithm was illustrated for STW SAR imaging.

This paper introduced the IRIS concept but more work is required to make it practical. Firstly, the probability map estimate for $P(x_i = 0|Y)$ was based on an estimate of the probability $P(x_i = 0|Z)$, where Z denotes the complete data in the EM algorithm. Using the EM framework it is possible to to obtain better approximations to the posterior probability which will translate into better estimates of the confidence image, i.e., the entropy of the probability map. Secondly, the reverse migration algorithm can be extended to fully 3D images. Thirdly, to obtain the final reconstructed image for the simulated example shown in the paper, we simply superimposed the scene reconstructions obtained at each iteration of IRIS. This can be improved by coupling the EM algorithm reconstructions over different IRIS iterations. Finally, as presented here, IRIS required human intervention, i.e., the placement of the virtual transmitter was manually determined by selecting regions of interest in the confidence map and looking at the information gain field images. The general IRIS procedure can be automated if good rules for region of interest selection can be developed.

References

[1] A. P. Dempster, N. M. Laird, and D. B. Rubin, "Maximum likelihood from incomplete data via the em algorithm," *Journal of Royal Statist. Soc. B*, vol. 39, pp. 1–38, January 1977.

[2] M. Figueiredo and R. Nowak, "An EM algorithm for wavelet-based image restoration," *IEEE Trans. on Image Processing*, vol. 12, no. 8, pp. 906–916, 2003.

[3] M. Ting, *Signal Processing for Magnetic Resonance Force Microscopy*. PhD thesis, Dept of EECS, Univ. of Michigan, Ann Arbor MI 48109-2122, May 2006.

[4] M. Ting, R. Raich, and A. O. Hero, "Sparse imaging using a sparse prior," in *Proc. IEEE Int. Conf. on Image Processing*, (Atlanta, GA), pp. 1261–1264, 2006.

[5] C. Cafforio, C. Prati, and F. Rocca, "SAR data focusing using seismic migration techniques," *IEEE Trans. on Aerosp. Electron. and Systems*, vol. 27, no. 2, pp. 194–206, 1991.

[6] R. Stolt, "Migration by Fourier transform," *Geophysics*, vol. 43, pp. 23–48, 1978.
[7] W. Carrara, R. Goodman, and R. Majewski, *Spotlight Synthetic Aperture Radar*. Boston: Artech House, 1995.
[8] W. Schmaedeke and K. Kastella, "Event-averaged maximum likelihood estimation and information-based sensor management," in *Proceedings of SPIE*, pp. 91–96, June 1994.
[9] K. Kastella, "Discrimination gain to optimize classification," *IEEE Transactions on Systems, Man and Cybernetics-Part A: Systems and Humans*, vol. 27, pp. 112–116, January 1997.
[10] C. Kreucher, K. Kastella, and A. O. Hero, "Multi-target sensor management using alpha-divergence measures," in *3rd Workshop on Information Processing for Sensor Networks*, (Palo Alto, CA), pp. 209–222, 2003.
[11] J. Marble and A. O. Hero, "Phase distortion correction for see-through-the-wall radar imaging," in *Proc. IEEE Int. Conf. on Image Processing*, (Atlanta, GA), pp. 2333–2336, 2006.